ELSEVIER

Thermochimica Acta 363 (2000) 37–45

thermochimica acta

www.elsevier.com/locate/tca

Thermogravimetric analysis of organic binder segregation during drying of particulate suspensions☆

Michael M. Mandanas*[,1], Gary L. Messing[2]

The Particulate Materials Center and Materials Research Laboratory, Pennsylvania State University, University Park, PA 16802, USA

Received 23 February 2000; received in revised form 20 June 2000; accepted 25 June 2000

Abstract

Thermogravimetric analysis (TGA) was used to evaluate microstructural evolution and binder segregation during drying of particulate suspensions of submicrometer alumina. The addition of 2 and 4 wt.% poly(vinyl alcohol) (PVA) binder decreased the evaporation rate by ~12 and ~20%, respectively, during the constant rate drying period. Increasing the PVA molecular weight (MW) extended the drying time also. At 4 wt.% addition, an acrylic emulsion binder did not affect the drying behavior but at 2 wt.% addition, the initial evaporation rate decreased by approximately 24%. It is shown that the TGA can be used to determine the drying stages of a particulate suspension during drying. © 2000 Elsevier Science B.V. All rights reserved.

Keywords: Drying; Binder; Segregation; Particulate; TGA

1. Introduction

Spray drying is routinely used to produce granules for automated pressing of ceramic parts [1–3]. An organic binder is typically added to the ceramic powder to induce viscoelasticity in the powder during pressing and also to develop green strength [1,4]. Non-uniform distribution of the organic binder in the spray dried granules can lead to microstructural defects during subsequent pressing, e.g. voids, which are difficult to remove during sintering. Such processing voids create fracture centers and reduce the strength of the fired body [1,2]. Other defects that have been related to organic binder segregation during spray drying include the formation of hollow and irregular granules [3]. These effects are well known in industry, but there are few studies on the origin of organic binder segregation during spray drying.

Zhang et al. [5–7] investigated the mechanisms of binder segregation in aqueous alumina (Al_2O_3)-polyvinyl alcohol (PVA) suspensions during drying. In their experiments, alumina slurries with varying amounts of PVA were dried in a beaker at different temperatures. Drying rates were monitored with a thermobalance and the dried disk was sectioned to determine the binder distribution in the axial direction. Zhang suggested that surface segregation results primarily from the competition between liquid migration/evaporation and polymer back-diffusion, and that it was primarily a function of PVA concentration and drying temperature. A one-dimensional numerical model was developed to account for solution flow between layers and binder concentration in the solu-

---

☆ Supported by the Particulate Materials Center, an NSF I/U CRC, Pennsylvania State University.

* Corresponding author. Tel.: +1-814-863-9904; fax: +1-8914-863-9704.
E-mail address: mmandanas@psu.edu (M.M. Mandanas).

[1] Member, The American Ceramic Society.

[2] Member, The American Ceramic Society.

0040-6031/00/$ – see front matter © 2000 Elsevier Science B.V. All rights reserved.

PII: S0040-6031(00)00591-8

tion, with the assumption that binder diffusion followed Fick's first law of diffusion. The resulting concentration gradient of PVA was assumed to result from back-diffusion counteracting binder flow in the solvent, consequently, decreasing the amount of segregation to the drying surface. In a later publication, Zhang et al. [8] demonstrated that binder adsorption limits its mobility, and consequently, limits segregation.

Soluble organic binders such as PVA are more mobile than colloidal binders such as latex and emulsion systems [9,10]. As demonstrated by Liang et al. [11], binder diffusion coefficients of PVA vary with specimen size, solution volume and temperature. Because these conditions vary during the drying process, it is important to know how binder diffusion changes as a function of different conditions and how these conditions change during the process. Because binder segregation is a potential problem in a number of applications, it would be useful to have an analytical tool to follow how the microstructure changes during drying and how suspension drying is affected by the presence of an organic phase. In this paper, we describe how binder segregation during drying can be evaluated by thermogravimetric analysis (TGA).

2. Experimental approach

2.1. Materials

High purity aluminum oxide (α-Al_2O_3)[3] was used as a model powder system for all of the experiments. The alumina particles were 0.6 μm in diameter and had a BET[4] surface area of 10.2 m^2/g. The organic binders selected for this study represent two of the major classes of binders used for dry pressing ceramics, i.e. (i) a solution type, PVA and (ii) an emulsion type, an acrylic emulsion[5]. The binders were stirred into the alumina slurry at pH ~8.8 after they had been stabilized with 0.2–0.5 wt.% (w/w Al_2O_3) ammonium polyacrylate[6] and an ammonium salt of polyacrylic acid[7], respectively. For the adsorption and rheological studies, dispersions were mixed in a 250 ml beaker with a magnetic stir bar. For the suspensions used for spray drying, a high-speed shear mixer[8] (800–1500 rpm) was used.

Two different grades of PVA were investigated: (i) molecular weight (MW) distribution of 31 000–50 000[9] and 87–88% hydrolyzed; and (ii) MW distribution of 124 000–186 000[10] and 87–88% hydrolyzed. Solutions of 15 and 20 wt.% PVA were prepared at room temperature in distilled water for the two grades of PVA [12]. The acrylic emulsion system was an aqueous dispersion of 43 wt.% solids at pH 9.0. The acrylic emulsion system had a size distribution of 85–110 nm.

2.2. Binder adsorption

Binder systems were added to 15 and 24 vol.% alumina slurries and stirred for 145 h at room temperature. For systems containing dispersants, the dispersant was added to the slurry and stirred for a few minutes before the binder was added. To determine the amount of binder adsorbed on the alumina particles, a small sample was centrifuged[11] for 105 min at 2000 rpm. The binder concentration in the supernatant was determined by gravimetric methods. The amount adsorbed on the particle surfaces was assessed by the difference between the initial and final concentration. The pH of the dispersions ranged from 9.0 to 9.2 throughout these experiments.

2.3. TGA of drying behavior

To investigate the effects of the organic binder on drying behavior, TGA[12] was used. A 10 mm diameter by 1 mm tall platinum pan was used as the sample

---

[3] A16-SG alumina, Alcoa Chemical, Bauxite, AR 72011, USA.

[4] Model Gemini 2375, VacPrep 061 Micromeretics Instruments, Norcross, GA 30093, USA.

[5] Duramax B-1020, Rohm and Hasas, Philadelphia, PA 19106, USA.

[6] Darvan 821A, R.T. Vanderbilt, Norwalk, CT 06855, USA.

[7] Duramax 3005, Rohm and Haas, Philadelphia, PA 19106, USA.

[8] LabMaster SI, Lightnin, a unit of General Signal, Rochester, NY 14602, USA.

[9] Airvol 205S, Air Products and Chemicals, Allentown, PA 18195, USA.

[10] Airvol 540, Air Products and Chemicals, Allentown, PA 18195, USA.

[11] Model CU-5000 Centrifuge, International Equipment, Needham Heights, MA 02194, USA.

[12] Model 2050 Thermogravimetric Analyzer, TA Instruments, New Castle, DE 19720, USA.

vessel. Approximately 150–300 mg of the suspensions was loaded in the TGA. Samples were heated at 60°C/min to 200°C and held isothermally until there was no observable change in weight (∼20 min). To evaluate rapid drying conditions, samples were isothermally heated by directly inserting them into a preheated TGA furnace at 200°C. For both experiments sample atmosphere was controlled via a purge gas connection to the furnace at 74 cm^3/min and to the balance at 29 cm^3/min.

To evaluate binder distribution in dried bodies, one-dimensional drying experiments were performed. Dispersions were poured into cylindrical vials ∼40 mm×10 mm (height×diameter) and dried for 48 h at ≈77°C. The dried bodies were sliced into ∼2 mm thick sections and the binder content was determined by heating a sample in air to 650°C.

2.4. Granule characterization

The suspensions were spray dried in a mixed flow, open cycle pilot plant spray dryer.[13] A pressure nozzle, with a 0.5 mm opening, was used with an inlet temperature of 250°C and an outlet temperature of 100°C. Chamber pressure was ∼120 mm H_2O and the nozzle pressure was maintained between 1.0 and 2.0 bar.

To evaluate binder segregation in spray dried granules, granules were microtomed and the PVA and emulsion binder was stained with ruthenium tetroxide, RuO_4.[14] Microtomed sections [13,14] of granules were collected on microscope slides and placed in a petri dish with BEEM® embedding capsules filled with ruthenium tetroxide, RuO_4. The dish was then quickly covered and sealed with paraffin wax. The sealed dish was placed in a black box and stored in a hood for a minimum of 30 h. The ruthenium tetroxide vapors specifically adsorb to the binder molecules and "map" their location [13]. These sections were then observed under an optical microscope.

3. Results and discussion

3.1. Binder adsorption

Table 1 shows the adsorption behavior of the PVA solution and the acrylic emulsion on the Al_2O_3 powder at room temperature. The relative amount of PVA adsorbed on the Al_2O_3 surface decreased as the amount of PVA added to the slurry increases, i.e. from ∼15% of the 2 wt.% PVA addition (3×10^{-4} g/m^2 Al_2O_3) to ∼8% of the 4 wt.% addition (3.6×10^{-4} g/m^2 Al_2O_3). The degree of adsorption for polymers such as PVA on solid surfaces is controlled mainly by the degree of polymerization, polymer concentration in solution, solvency and net adsorption energy [15,16]. PVA adsorption decreased to ∼1.2×10^{-4} and ∼1.6×10^{-4}, respectively, in the presence of the ammonium polyacrylic acid dispersant. It is the number of available sites on the alumina surface that determine how much binder is adsorbed. That is, the dispersant reduced the number of available sites available for binder adsorption [16,17].

For the acrylic emulsion, ∼12% adsorbed at a binder addition of 3 wt.% and ∼8% adsorbed at a binder addition of 5 wt.%, 3.6×10^{-4} and 4.0×10^{-4} g/m^2 Al_2O_3, respectively. Emulsion adsorption can also decrease with the addition of the dispersant. At 3 wt.% addition, the adsorbed binder decreased to 2.7×10^{-4} g/m^2 Al_2O_3 while at 5 wt.% addition, the adsorbed amount was 4.0×10^{-4} g/m^2 Al_2O_3.

The interaction of an acrylic binder with an alumina surface is through ionized acid sites. Lower binder pK_a, <7.0, values indicate the presence of more acid sites while higher pK_a values indicate fewer sites. Berry et al. [18] showed that the extent of adsorption

Table 1
Binder adsorption of organic binders in 10 vol.% Al_2O_3 suspensions[a]

	2 wt.%	3 wt.%	4 wt.%	5 wt.%
PVA (205s)	3.0		3.6	
PVA (205s)+Darvan 821A	1.2		1.6	
Acrylic emulsion (Duramax B1020)		3.6		4.0
Acrylic emulsion+ Duramax 3005		2.7		4.0

[a] Total binder added ($\times10^{-4}$ g (binder)/m^2(Al_2O_3)).

---

[13] Model Pilot Spray Dryer 5, APV Anhydro Separation Tech., Tonawanda, NY 14150, USA.

[14] Electron Microscopy Sciences Cat No. 20700-05, Ft. Washington, PA 19034, USA.

for acrylic emulsion binders changes as a function of the dispersant acid number. A higher acid number corresponds to a higher affinity for the powder surface resulting in fewer available sites for binder adsorption. The acid number of the acrylic acid homopolymer dispersant is 8.6 and is a relatively high number compared to 7.0 for the binder [19]. Therefore, the low degree of adsorption of the acrylic emulsion binder can also be attributed to preferential adsorption of the dispersant.

3.2. Binder distribution during drying

Fig. 1 summarizes the relationships between binder type and distribution measured during the one-dimensional drying experiments. Surface segregation of the binder was observed for the 4 wt.% PVA addition to a 10 vol.% Al_2O_3 suspension while there was little binder segregation when 2 wt.% PVA was added to a 30 vol.% Al_2O_3 suspension. The difference in PVA segregation can be attributed to the drying time before the particle network forms. During the constant rate period, the binder migrates with the solution and collects at the surface until a particle network forms at which time shrinkage stops and the falling rate drying period begins. At a low solids concentration, the constant rate period of drying is longer since more liquid must evaporate before the particulate suspension reaches the critical solids concentration, i.e. percolation limit. At a higher solids content, the solids concentration approaches the critical volume concentration required for constriction of the floc structure of the particle network and therefore, a shorter constant rate period is observed. Once the percolated network forms, the PVA binder must diffuse and migrate through the tortuous particle network, i.e. permeability decreases. Consequently, binder segregation becomes a function of permeability through both the particle network and the binder solution distributed throughout the body.

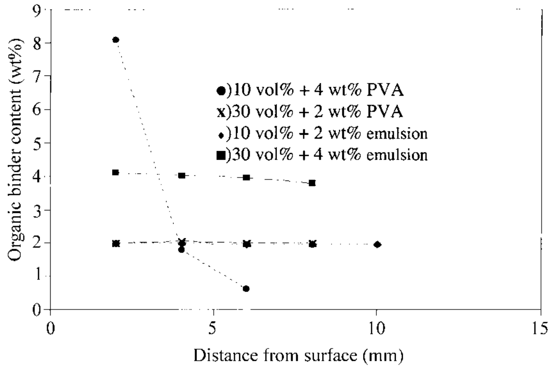

Fig. 1. Binder distribution in one-dimensionally dried samples.

In suspensions containing the acrylic emulsion, binder distribution is relatively constant throughout the body for both high and low solids concentration slurries. This can be explained considering the size of the acrylic particles. The emulsion droplet size is comparable to the alumina particle size, ~100 vs. 500 nm. Additionally, emulsion droplets can coalesce into larger droplets during drying [20,21]. Bergna [22] proposed and demonstrated that when one fraction of the particles is significantly smaller, 7–200 nm than the coarser particles, 0.5–10.0 μm, then the smaller particles can segregate to the surface by diffusion with the liquid. Consequently, for emulsion binders to segregate, they must be sufficiently small to migrate easily through the suspension particle network.

3.3. Drying kinetics

The drying behavior of a 10 wt.% suspension heated at 60°C/min to 200°C in a TGA is shown in Fig. 2a. Part I of the drying curve represents the stage where the suspension approaches equilibrium with the drying environment. Initially, as the TGA temperature increases, moisture is lost at the surface and the rate of weight loss rate increases until the equilibration temperature between the body and the corresponding furnace environment is reached, i.e. wet-bulb temperature. At a furnace temperature of ~200°C with a relative humidity of ~4.0%, $T_{\text{wet-bulb}}$ is ~90°C while at a relative humidity of ~0.1%, $T_{\text{wet-bulb}}$ is ~50°C [23]. Part II of the curve is the constant rate drying period which is the stage where the evaporation occurs at the liquid/air interface of the slurry and water is readily available at the surface. Part III is the falling rate drying period which occurs when the evaporation front moves into the body, and liquid cannot flow to the surface.

The other plot in Fig. 2a shows the drying behavior of a suspension dried isothermally. The slurry was introduced into the TGA furnace, after it was preheated to 200°C, to more closely simulate spray drying

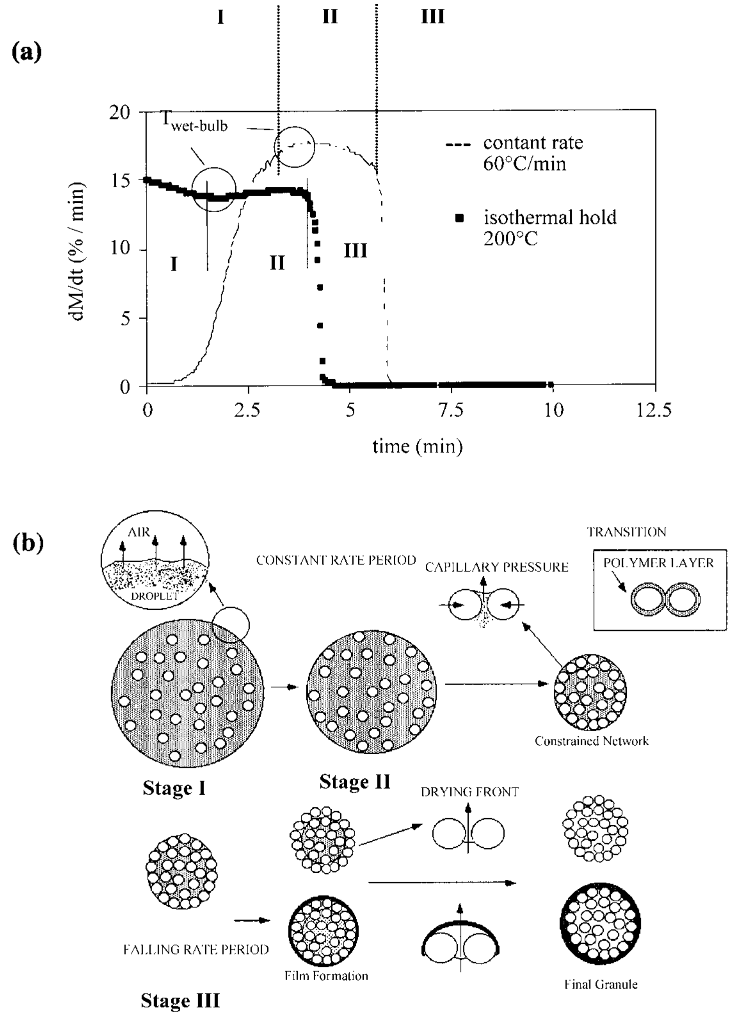

Fig. 2. (a) Typical drying curves for 10 vol.% Al_2O_3 suspensions, (b) Schematic of the microstructural evolution during drying of a particulate suspension droplet.

conditions. Sections II and III of plot b, represent the constant rate and falling rate periods of drying. The drying curves from the isothermal experiments are more similar in appearance to the classical drying curves where equilibrium is reached quickly followed by a relatively flat evaporation rate, i.e. constant rate period, before proceeding into the falling rate period of drying. Although the two curves presented appear different, they represent the relative drying rates and can be used to compare the drying behavior as a function of suspension parameters.

It is informative to consider the microstructural evolution of a particulate suspension during drying, with particular reference to spray dried droplets. There is approximately 1–2 orders of magnitude (depending on droplet size) difference in the surface to volume ratio between the TGA sample vessel and a droplet, i.e. difference in time scales. However, the drying stages are similar and therefore, drying and binder behavior can be qualitatively evaluated. Initially, particles are suspended in a liquid and thus liquid is readily available at the surface during the initial stage of drying. As water evaporates, the droplet shrinks and the particles crowd closer together. The droplet continues to shrink until it reaches a constrained state where moisture can only be drawn to the surface by capillary forces. At this stage, the body is under a capillary hydrostatic pressure. For further drying, the evaporation front moves into the body and the drying rate decreases. Moisture can be removed only through vapor diffusion within the particle network.

Fig. 2b shows the relation between the isothermal TGA plots and the microstructural evolution of a particulate suspension. The droplet is used as an example of how the TGA plots can monitor particle movement and binder migration during drying. From the weight loss data, the solids concentration within the body can be determined for each section of the drying plot and the stages of drying can be quantified. In a majority of the experiments, the change in slope from the constant rate period to the falling rate period corresponded to a range in solids concentration of ~45–62 vol.%. The significance of this parameter will be addressed for each slurry parameter investigated. Of interest in this paper is the effect of binder addition on the drying stages. In particular, the duration of each stage and the critical concentrations required to transition to the next drying stage.

Fig. 3 compares the drying rate of alumina suspensions containing 10 vol.% vs. 30 vol.%. Initially, the drying curves for the two suspensions behave similarly showing a gradual increase in evaporation rate up to the equilibration point. The slurry that started with 10 vol.% solids plateaus into a constant rate period before transitioning to the falling rate period. In contrast, in the suspension starting with a higher solids content, a short constant rate period is followed by a rapid increase in the drying rate prior to the transition into the falling rate period. At the transition stage from the constant rate to the falling rate, the 30 vol.% slurry had dried to ~45 vol.%. After the same period of time, the 10 vol.% slurry was at ~13.5 vol.%. The more rapid heating leads to the eruption of the surface region in the more highly concentrated suspension resulting in suspension boiling represented by the spike in the drying rate. The 10 vol.% slurry does not reach ~45 vol.% until later in the drying curve where a transition from the constant rate period to the falling rate period is observed.

Fig. 4a illustrates the effect of PVA on the drying rate of a 10 vol.% suspension. In the presence of PVA binder, the initial evaporation rate decreases and the

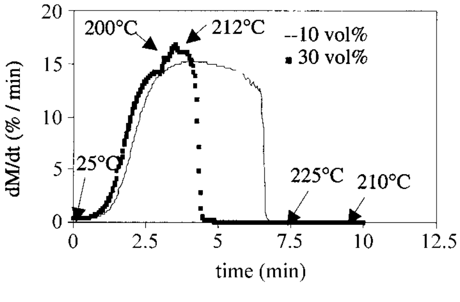

Fig. 3. Comparison of the drying behavior of alumina suspensions with different concentrations (furnace temperatures are indicated).

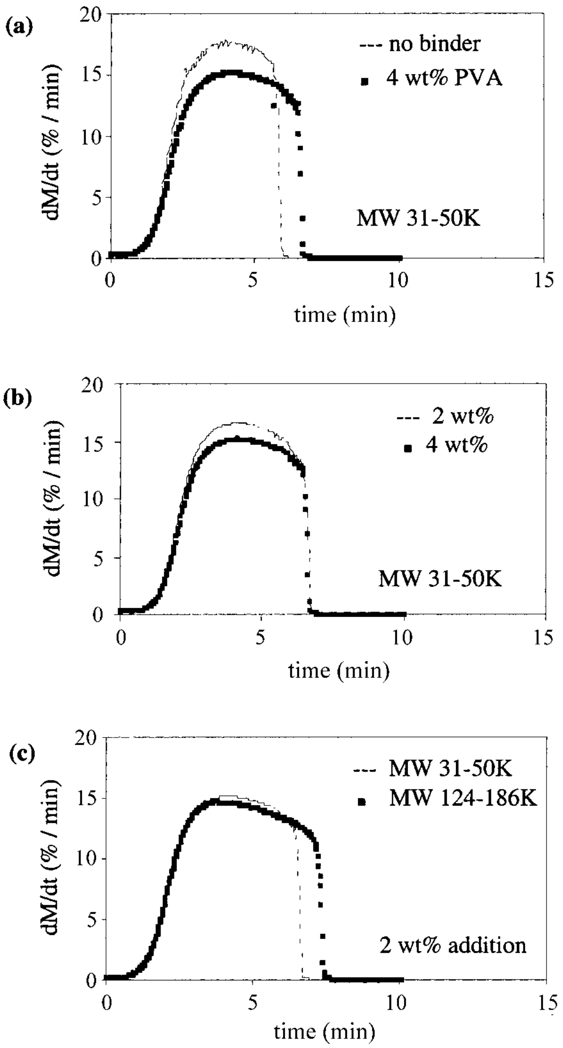

Fig. 4. Drying behavior of 10 vol.% Al_2O_3 suspensions with PVA solution binder.

drying period is extended. These effects are attributed to PVA segregation to the surface. As discussed earlier, the duration of the constant rate period is a function of solids loading. However, if a surface barrier layer has formed because of binder segregation, then drying during the constant rate period becomes a function of the permeability of the organic binder. The transition from the constant rate period to the falling rate period corresponded to an alumina concentration of ~42 vol.% and a PVA concentration of ~16 vol.%. The ~3 vol.% decrease in the alumina concentration necessary for the onset of the falling rate period can therefore be attributed, at least in part, to the presence of a soluble binder.

Fig. 4b compares the drying behavior of 10 vol.% alumina suspensions containing 2 and 4 wt.% PVA. Similar drying times were observed which suggests that surface permeability of the segregated binder is either not affected or was affected in the same manner. However, the initial drying rate for the 2 wt.% sample was less than for the 4 wt.% sample. This can be related to the change in the solution viscosity during drying. The viscosity, at room temperature, for a 2 wt.% solution is ~3 and ~7 mPa s for a 4 wt.% solution [12]. During the initial period of drying, PVA diffuses to the surface. As drying continues, the solution viscosity increases and the diffusivity of PVA decreases. The barrier layer at the surface is more easily formed at lower initial PVA concentrations since the film takes longer to form at these lower PVA concentrations.

Fig. 4c illustrates the effect of PVA MW on the drying behavior of a 10 vol.% suspension. The constant rate period extends with increasing MW. Once PVA has migrated to the surface, the evaporation rate becomes a function of surface permeability. With longer polymer chains, i.e. MW 124–186 K>MW 31–50 K, chain entanglement increases and as a result, the surface barrier layer becomes less permeable. Although viscosity also increases with MW, it is the concentration of the polymer at the surface that is critical. That is, as long as the surface layer remains permeable, i.e. below the critical film formation concentration, drying time is a function of the permeability of the surface layer which in general decreases as MW increases [24]. It has also been suggested that the ability of the polymer to reach the surface is a function of MW [25].

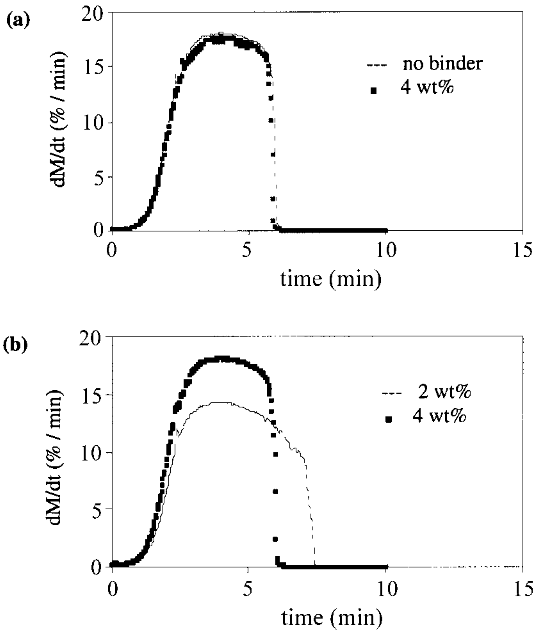

Fig. 5. Drying behavior of a 10 vol.% Al_2O_3 suspensions with an acrylic emulsion binder.

Fig. 5a compares the drying behavior of a 10 vol.% alumina suspension with and without an acrylic emulsion binder. At 4 wt.% addition of the acrylic emulsion binder there were no effects on the drying curve and it is similar to the drying curve of an alumina suspension with no binder. Interestingly, decreasing the binder concentration to 2 wt.%, Fig. 5b, lowers the initial drying rate and extends the drying time, i.e. surface segregation is implied. The probability of droplets encountering each other at a 2 wt.% addition is lower relative to a 4 wt.% addition. Therefore, the time-period that emulsion droplets remain as discrete 100 nm droplets is longer at lower concentrations. The kinetics of flocculation and coalescence have been related to emulsion concentration [21]. As 100 nm droplets, the emulsion droplets can readily diffuse through the pore network of the 500 nm Al_2O_3 particles. Once droplets reach the surface, coalescence can occur and a barrier layer can form which decreases the permeability for moisture removal. However, at a 4 wt.% addition, the droplets can more readily coalesce into larger droplets. Larger droplets can be formed early in the drying process and can be

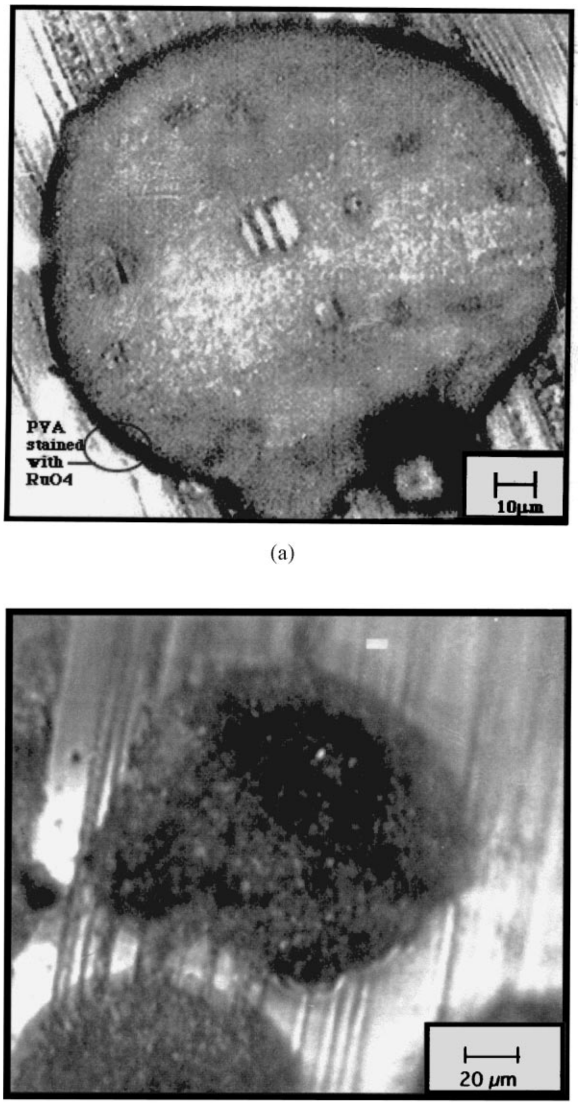

(a)

(b)

Fig. 6. Optical micrograph of a microtomed section of a spray dried granule with (a) 4 wt.% PVA and (b) 4 wt.% emulsion binder. The dark sections are rich in binder and have been stained with RuO_4.

constrained by the network structure formed by the 500 nm Al_2O_3 particles. The transition period to the falling rate period of the sample with 2 wt.% emulsion occurred at ~39 vol.% Al_2O_3. The lower alumina concentration required for the transition suggests that the emulsion droplets segregated to the surface and formed a barrier layer resulting in a decrease in the drying rate. On the other hand, the transition period for the 4 wt.% emulsion addition occurred at ~50 vol.%, which is represented by the small decrease in evaporation rate. Although an increase in the critical alumina concentration is observed, the similar drying curve suggests a drying behavior that is similar to an alumina suspension with no binder.

3.4. Microscopy

Fig. 6a shows a microtomed section of a granule spray dried from a ~55 wt.% Al_2O_3 suspension containing PVA that was preferentially stained black by ruthenium tetroxide. The distribution of the reacted area confirms that for 4 wt.% initial PVA content, the PVA is primarily concentrated in the surface/near-surface region of the granule after spray drying. Additionally, the micrograph shows that the binder is distributed uniformly around the granule with sharp concentration gradient towards the inside of the granule. Fig. 6b shows a microtomed section of a granule produced from a ~55 wt.% Al_2O_3 suspension containing 4 wt.% acrylic emulsion binder. The distribution of the stained regions indicates that the emulsion binder is distributed throughout the granule. These results agree well with the conclusions derived from the TGA experiments.

4. Conclusions

It has been demonstrated that the TGA is a useful analytical tool for investigating and interpreting the drying behavior of particulate suspensions containing organic additives. Using the TGA, slurry parameters (solids loading, binder type, binder concentration and MW) were shown to have significant effects on the microstructural evolution and organic binder segregation of particulate suspensions during drying. The development of the TGA approach offers several advantages (1) requires less material and time (2) provides the formulator with a means of evaluating binder segregation and (3) it is independent of the operator. This allows for a systematic evaluation of the interactions between the slurry components involved and can provide insight on the drying behavior of particulate suspensions.

Acknowledgements

The authors would like to acknowledge the Particulate Materials Center for providing the financial support for this research project. We would also like to thank Rosemary Walsh at the EM Facility for Life Sciences, The Life Sciences Consortium and Biotechnology Institute at The Pennsylvania State University for helpful discussions during the preparation of the microtomed samples.

References

[1] J. Reed, Principles of Ceramic Processing, 2nd Edition, Wiley, New York, 1995.
[2] S.J. Lukasiewicz, Spray-dried ceramic powders, J. Am. Ceram. Soc. 72 (4) (1989) 617–624.
[3] F. Shaw, Spray drying: a traditional process for advanced applications, Ceram. Bull. 69 (9) (1990) 1484–1489.
[4] S.J. Lukasiewicz, J.S. Reed, Character and compaction response of spray dried agglomerates, Ceram. Bull. 57 (9) (1978) 798–801.
[5] Y. Zhang, N. Uchida, K. Uematsu, Direct observation on non-uniform distribution of PVA binder in alumina green body, J. Mater. Sci. 30 (1995) 1357–1360.
[6] Y. Zhang, X. Tang, N. Uchida, K. Uematsu, Mathematical simulation for segregation of PVA during drying, J. Ceram. Soc. Jpn., Int. Ed. 101 (2) (1993) 177–180.
[7] Y. Zhang, X. Tang, N. Uchida, K. Uematsu, Binder surface segregation during spray drying of ceramic slurry, J. Mater. Res. 13 (7) (1998) 1881–1887.
[8] Y. Zhang, T. Suga, M. Kawasaki, X. Tang, N. Uchida, K. Uematsu, Effect of poly(vinyl alcohol) adsorption on binder segregation during drying, J. Am. Ceram. Soc. 79 (2) (1996) 435–440.
[9] T. Patton, Paint Flow and Pigment Dispersion, 2nd Edition, Wiley, New York, 1979.
[10] S.X. Pan, H.T. Davis, L.E. Scriven, Modeling moisture distribution and binder migration in drying paper coatings, Tappi J. 78 (8) (1995) 127–142.
[11] Z. Liang, Y. Zhang, N. Uchida, K. Uematsu, Diffusion of polymeric binder in alumina powder compact in a low pH range, J. Mat. Sci. Lett. 14 (1995) 1610–1612.
[12] Air Products, Airvol® Polyvinyl Alcohol, Solution Preparation Guidelines, Product Literature, 1997.
[13] L.C. Sawyer, D.T. Grubb, Polymer Microscopy, Chapman & Hall, New York, 1994, pp. 104–109.
[14] P. Gray, The Microtomist's Formulary and Guide, Blakiston, NY, 1954.
[15] M.A. Cohen-Stuart, T. Graule, L. Gauckler, Experimental aspects of polymer adsorption at solid/solution interfaces, Adv. Colloid Interf. Sci. 24 (1986) 143–239.
[16] J. Cesarano III, I. Aksay, Stability of aqueous α-Al_2O3 suspensions with poly(methacrylic acid) polyelectrolyte, J. Am. Ceram. Soc. 71 (4) (1988) 250–255.
[17] P.C. Hidber, T.J. Graule, L.J. Gauckler, Competitive adsorption of citric acid and poly(vinyl alcohol) onto alumina and its influence on the binder migration during drying, J. Am. Ceram. Soc. 78 (7) (1995) 1775–1780.
[18] A. Berry, L. Bogan, S. Agostine, Adsorption of organic additives on powder surfaces, Ceram. Trans. 62 (1995) 125–132.
[19] D. Lide (Ed.), CRC Handbook of Chemistry and Physics, 72nd Edition (special student edition), CRC Press, Boca Raton, FL, 1992.
[20] S. Rakers, L. Chi, H. Fuchs, Influence of the evaporation rate on the packing order of polydisperse latex monofilms, Langmuir 13 (1997) 7121–7124.
[21] R. Borwankar, L. Lobo, D. Wasan, Emulsion stability — kinetics of flocculation and coalescence, Colloid. Surf. 69 (1992) 135–146.
[22] H.E. Bergna, Method of making maleic anhydride, US Patent 4,677,084 (1985).
[23] D.W. Green (Ed.), Perry's Chemical Engineering Handbook, 7th Edition, McGraw-Hill, New York, 1997.
[24] P.J. Flory, Principles of Polymer Chemistry, Cornell University Press, Ithaca, NY.
[25] A. Hariharan, S. Kumar, T. Russell, A lattice model for the surface segregation of polymer chains due to molecular weight effects, Macromolecules 23 (1990) 3584–3592.